# Characterization of Mineral Targets by Laser Desorption and Ionization in Preparation of the MOMA Investigation Onboard the ExoMars-2018 Rover

Walter Goetz, Ricardo Arevalo, Veronica Pinnick, Ryan Danell, Stéphanie Getty, M. Oehlke, H. John, X. Li, A. Grubisic, W. Brinckerhoff, et al.

**CHARACTERIZATION OF MINERAL TARGETS BY LASER DESORPTION AND IONIZATION IN PREPARATION OF THE MOMA INVESTIGATION ONBOARD THE EXOMARS-2018 ROVER.**

W. Goetz[1], R. Arevalo Jr.[2], V. Pinnick[2], R. Danell[3], S. Getty[2], M. Oehlke[1], H. John[1], X. Li[2], A. Grubisic[2], W. Brinckerhoff[2], H. Steininger[1], F. Goesmann[1], S. Siljeström[4], F. Raulin[5], C. Szopa[6], A. Buch[7], and the MOMA Science Team[1-10], [1]MPS, Justus-von-Liebig-Weg 3, 37077 Göttingen, Germany (goetz@mps.mpg.de), [2]NASA GSFC, Greenbelt, MD, USA, [3]Danell Consulting, Winterville, NC, USA, [4]SP Techn. Res., Borås, Sweden, [5]LISA, U. Paris-Est, Creteil, France, [6]LATMOS, Guyancourt, France, [7]LPGM, Ecole Centrale Paris, Chatenay-Malabry, France, [8]U. Bremen, Germany, [9]U. Nice, France, [10]INAF - Astrophysical Observatory of Arcetri, Firenze, Italy.

**Introduction:** The MOMA instrument (Mars Organic Molecule Analyzer [1]) onboard the ESA-Roskosmos led ExoMars-2018 rover mission shall investigate Martian near-surface samples by Laser Desorption and Ionization (LDI). This experimental technique uses UV laser impact to ablate molecular fragments that shall be analyzed by mass spectrometry and is thus geared towards characterization of the *organic* inventory in Martian subsurface samples. Here we present an end-to-end LDI experiment performed on a small (though diverse) set of terrestrial inorganic samples (minerals). The experiment has the following goals: (1) explore the possibility to identify minerals by LDI, (2) characterize the physical interaction between laser and mineral by measuring the average mass of ablated material per laser shot, and (3) present data acquired by the MOMA engineering test unit (ETU) at NASA GSFC. The recorded mass peaks are part of the "background" that will be encountered during any in situ measurement on the surface of Mars and in which peaks of organic compounds are embedded. Hence such data contribute to a reference data set that will be important to interpret complex spectra of any organic-bearing sedimentary rocks on Mars.

**Samples:** Four samples were chosen for these experiments: magnetite (Ward's Science XRD & microprobe standard), gypsum (Red River Floodway, Winnipeg, MB, Canada), quartz within granite (south svecofennian granite, north of Västervik, Sweden), and olivine (ultramafic nodule within tertiary basalt, Lower Saxony, Germany). These samples were prepared as ~20 µm thick thin sections (Fig. 1) and represent a significant subset of global Martian surface minerals (oxides, sulfates, silica & silicates). We are not reviewing here their global occurrence, but address – as an example – their occurrence along the traverse of the Curiosity rover in Gale crater: Magnetite and olivine have strongly varying abundances up to, respectively, 13 and 16 wt% of a bulk sample (including amorphous part) [2-4]. Gypsum is not commonly found, but calcium sulfate veins (anhydrite or bassanite [5]) are ubiquitous. Quartz is an accessory mineral (~1 wt%) in most samples [2-4], but high amorphous silica has been detected at various places [4, 6].

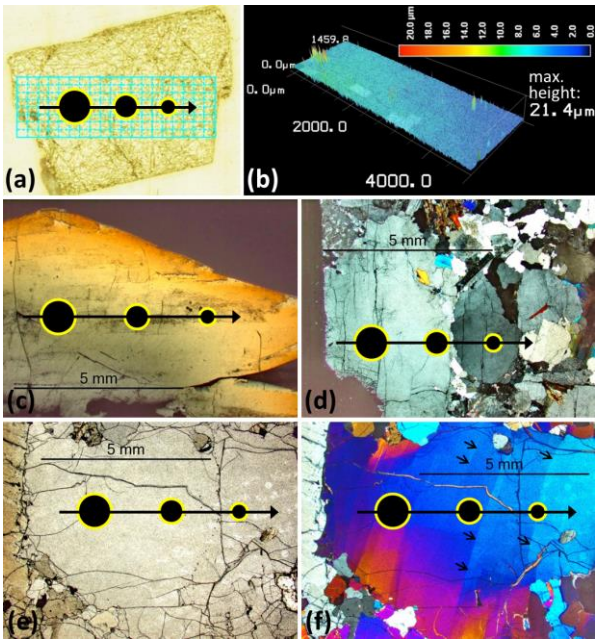


***Fig. 1:*** *Mineral samples chosen for the LDI experiment: (a) Magnetite. The light blue grid (4.8 * 1.4 mm) is used to characterize the surface state of the area (presented in 3D view in b) that will contain the laser shots. (c) Gypsum as seen in transmission with crossed polarizers. Yellow-reddish colors near the border indicate increased thickness. (d) Quartz crystals (different gray tones reflecting different crystallographic orientations) in transmitted light (crossed polarizers). (e-f) Olivine crystal (>5 mm across) in transmitted light without (e) and through crossed polarizers (f). Differently oriented fractures crosscut the crystal. Gradual color change from blue to purple and orange (in f) is caused by thinning of the crystal. Black arrows indicate deformation lines with subgrain misorientation of some degrees (also suggested by color pattern). The black filled circles in all panels (except b) represent a decreasing number of shots from left to right (leftmost location is referred to as 'marker spot'). The areas of all samples were characterized as shown in (b).*

**Experimental setup:** Both setup and measurement protocol are fairly close to the ones envisioned for flight: The UV laser pulse ($\lambda$ = 266 nm, $\tau$ ~ 1.3 ns) hits the sample at an incident angle of 45° and probes

~0.3x0.6 mm of that sample surface (placed at laser focus). The laser pulse intensity is slowly ramped up (15-150 μJ, or roughly 0.01-0.1 J/cm$^2$) until a stable MS signal is obtained. The mass spectrometer, consisting of a Linear Ion Trap (LIT), ejects radially organic and inorganic ions based on mass-to-charge (m/z) ratios across a mass range of 50-1000 Da. The LIT can be operated in SWIFT mode (Stored Waveform Inverse Fourier Transform) in order to selectively enrich a subset of masses (within a narrower m/z range) out of the primary (broad) distribution of masses.

**LDI spectra:** The following laser shot protocol was applied (from left to right, see e.g. Fig. 1a): 1000 shots (marker spot), 500, and 100 shots. Average mass spectra were saved for 10 subsequent shots. Fig. 2 shows an example LDI spectrum for olivine, including mass assignments for inorganic peaks. Interestingly, laser coupling with quartz was so poor that no clear ablation pit was identified via microscopic examination; however, significant thermal fracturing and evidence for an ablation condensate blanket can be seen at the site of the marker spot.

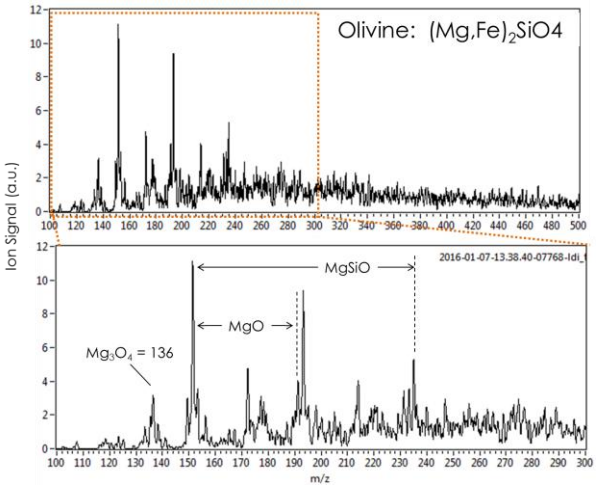


***Fig. 2*** *Laser desorption/ionization mass spectrum for olivine thin section, showing evidence for metastable elemental clusters characteristic of forsteritic olivine composition.*

**Ablation of samples:** Coupling between incident laser light and the sample substrate is controlled by the parameters of the laser radiation and the physicochemical properties of the targeted material. As the parameters of the MOMA laser were held constant during this experiment (with exception of energy versus sample), the ablation threshold for each mineral explored here depends on its respective chemical composition, optical transparency and microtexture.

The power profile of the laser beam contains several distinct "hot spots," characterized by higher local fluences than the average, that ablate material within an area much smaller than the area of illumination (beam ellipse of 0.3 x 0.6 mm, see above). Fig. 3 presents the laser pit holes generated by 1000 laser shots collected on each mineral. The morphology of these holes is remarkably different in size and shape. As seen below, the optical transparency of gypsum and especially quartz resulted in: limited absorption of the incident radiation; localized heating of incubation centers (e.g., crystallographic defects) within each grain; and, ultimately thermal crack propagation. In contrast, the marker spots for magnetite and olivine show more characteristic elliptical ablation pits.

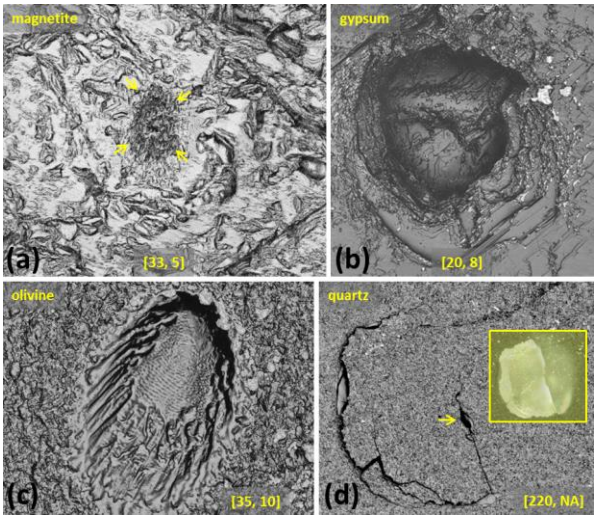


***Fig.3*** *Morphology of laser pit holes (after 1000 shots) for the samples presented in Fig.1. Laser-generated feature in (a) is marked by arrows. Diameter and depth of laser-generated features (specified, respectively, in each panel in μm) depend considerably on the mineral type. (c). Fracturing of gypsum (b, with visible Wallner lines) and quartz (d, with clear crack tip opening displacement) resulted from thermal stress due to high transparency/low absorption of the 266 nm radiation. Images (a) – (b) have been generated by "shape from shading" (for illumination by a laser beam, part of confocal laser microscope, Keyence Inc.). The small inset in (d) is the visible microscope image that shows that the "visible feature" (ablation condensates?) is approximately circular, although the topography is not.*

**References:** [1] Goetz W. et al. (2011) EPSC-DPS, 6, Nantes, France. [2] Cavanagh P. D. et al. (2015) LPSC, #2735. [3] Treiman A. H. et al. (2015), LPSC, #2620. [4] Morris R. V. et al. (2016) LPSC. [5] Rapin W. et al. (2015), LPSC, #2966. [6] Frydenvang J. et al. (2016), LPSC.